

12 March 2018

**SEX-DEPENDENT DIFFERENCES IN SPONTANEOUS AUTOIMMUNITY IN ADULT
3xTG-AD MICE**

Minesh Kapadia¹, M. Firoz Mian², Bernadeta Michalski¹, Amber Azam⁵, Donglai Ma³,
Patrick Salwierz⁴, Adam Christopher⁴, Elyse Rosa¹, Iva Zovkic⁵, Paul Forsythe², Margaret
Fahnestock¹, and Boris Sakic¹

¹Dept. of Psychiatry and Behavioral Neurosciences,

²Dept. of Medicine,

³Dept. of Pathology and Molecular Medicine,

⁴Biochemistry and Bachelor of Health Sciences Undergraduate program

McMaster University, Hamilton, ON, Canada

⁵Dept. of Psychology, University of Toronto Mississauga,
Mississauga, ON, Canada

Running title: Sex-dependent immune changes in 3xTg Mice

- Abstract Word Count: 282
- Manuscript Word Count: 5069
- Figures, Tables: 6
- References: 78

Correspondence:

Boris Sakic, Ph.D.

Department of Psychiatry and Behavioral Neurosciences, McMaster University

Psychology Building Rm. 303

1280 Main St. West, Hamilton, Ontario, Canada L8S 4K1

tel.: (905) 518-7833

e-mail: sakic@mcmaster.ca

Abstract The triple-transgenic (3xTg-AD) mouse strain is a valuable model of Alzheimer's disease (AD) because it develops both amyloid-beta ($A\beta$) and tau brain pathology. However, 1-year-old 3xTg-AD males no longer show plaques and tangles, yet early in life, they exhibit diverse signs of systemic autoimmunity. The current study aimed to address whether females, which exhibit more severe plaque/tangle pathology at 1 year of age, show similar autoimmune phenomena and if so, whether these immunological changes coincide with prodromal markers of AD pathology, markers of learning and memory formation and epigenetic markers of neurodegenerative disease. Six-month-old 3xTg-AD and wild-type mice of both sexes were examined for T-cell phenotype ($CD3^+$, $CD8^+$ and $CD4^+$ populations), serological measures (autoantibodies, hematocrit), soluble tau/phospho-tau and $A\beta$ levels, brain-derived neurotrophic factor (BDNF) expression, and expression of histone H2 variants. Although no significant group differences were seen in tau/phospho-tau levels, 3xTg-AD mice had lower brain mass and showed increased levels of soluble $A\beta$ and downregulation of BDNF expression in the cortex. Splenomegaly, depleted CD^+ T-splenocytes, increased autoantibody levels and low hematocrit were more pronounced in 3xTg-AD males than in females. Diseased mice also failed to exhibit sex-specific changes in histone H2 variant expression shown by wild-type mice, implicating altered nucleosome composition in these immune differences. Our study reveals that the current 3xTg-AD model is characterized by systemic autoimmunity that is worse in males, as well as epigenetic changes of unknown origin. Given the previously observed lack of plaque/tangle pathology in 1-year-old males, an early, sex-dependent autoimmune mechanism that interferes with the formation and/or deposition of aggregated protein species is hypothesized. These results suggest that more attention should be given to studying sex-dependent differences in the immunological profiles of human patients.

Keywords: Alzheimer's disease, 3xTg-AD mice, autoantibodies, T-lymphocytes, protective autoimmunity, soluble amyloid-beta, tau protein, BDNF, histone variants.

Abbreviations: 3xTg-AD, triple-transgenic model of AD; AD, Alzheimer's disease; APC, allophycocyanin; A β , amyloid-beta; ANA, anti-nuclear antibody; BDNF, brain-derived neurotrophic factor; dsDNA, double-stranded DNA; CD, cluster of differentiation; ELISA, enzyme-linked immunosorbent assay; FITC, fluorescein isothiocyanate; HRP, horseradish peroxidase; MCI, mild cognitive impairment; PBS, phosphate-buffered saline; PE, phycoerythrin; qRT-PCR, quantitative reverse transcription polymerase chain reaction; TBS, tris-buffered saline; WT, wild-type.

1. Introduction

Alzheimer's disease (AD) is an age-related, neurodegenerative disorder that disproportionately affects women, both in prevalence and severity [1, 2]. The causes of this sex discrepancy remain poorly understood but may involve risk factors beyond longevity, including genetic and functional variations between females and males [3-6]. Frequently reported functional imbalances in patients' immune system suggest that immunity plays an important role in the etiology of AD [7] and support immunization as a promising treatment strategy [8]. However, progress has been hampered by the lack of an appropriate animal model in which cause-effect relationships can be studied in a controlled, systematic manner. This has made it difficult to elucidate whether immune cell activation reflects a neuropathogenic or alternatively, a brain reparative process.

Triple-transgenic 3xTg-AD (*PS1_{M146V}*, *APP_{swe}*, *tau_{P301L}*) mice have proven to be an invaluable tool for studying the etiology, pathogenesis, and treatment of AD [9]. This is primarily due to evidence of age-related learning/memory deficits that emerge in parallel with intraneuronal pathology around 4 months of age, and the aggregation of amyloid-beta ($A\beta$) plaques and neurofibrillary tangles in the cortex and hippocampus between 12 and 15 months of age [10, 11]. In this model, soluble $A\beta$ precedes and contributes to the accumulation of tau pathology [12, 13], and inflammation potentiates neuropathology [14-16]. However, little effort has been made to assess behavioral changes in the context of immunity. In 3xTg-AD males, we observed that behavioral deficits similar to mild cognitive impairment (MCI) appear as a prodrome to subsequent age-related decline in spatial learning/memory performance [17]. In particular, these mice display anxiety-like behaviors (e.g., "acrophobia" in the step-down test, thigmotactic response in a swimming pool), altered olfactory discrimination, and impaired "cognitive flexibility" in reversal

trials of the water maze within the first 6 months of life. More complex performance deficits in learning/memory tasks develop between 6 and 12 months, yet not a full-blown AD-like “dementia.” Behavioral alterations are accompanied by age-dependent increases in autoimmune manifestations that include splenomegaly, elevated serum autoantibody levels, low hematocrit and reduced numbers of CD4⁺/CD8⁺ T-cells. Most importantly, the brains of these 1-year-old males do not show AD-like neuropathology [17]. This loss of AD phenotype was independently confirmed by the donating investigator (<https://www.jax.org/strain/004807>) and contrasts with the pronounced A β and tau pathology in 1-year-old 3xTg-AD females [18].

This sex-dependent shift is interesting in light of recent reports suggesting that male 3xTg-AD mice perform worse than females on learning/memory tasks at 6 months of age [19, 20]. Given these sex differences in behavioral performance and plaque/tangle pathology at later ages, the present study was designed to examine whether 6-month-old 3xTg-AD males and females exhibit similar discrepancies in the severity of autoimmune manifestations, in the levels of soluble AD-associated protein species, and in the expression of markers related to learning/memory and to epigenetic alterations in neurodegeneration. We assayed T-cell phenotype (CD3⁺, CD8⁺ and CD4⁺ populations), serological measures (autoantibodies, hematocrit), prodromal AD markers (soluble tau/phospho-tau and A β), brain-derived neurotrophic factor (BDNF) mRNA, and histone H2 variant expression in the cortex, thus revealing cellular/molecular targets for future mechanistic studies.

2. Methodology

2.1. Animals

Colonies of homozygous 3xTg-AD mice (*PS1*_{M146V}, *APP*_{swe}, *tau*_{P301L}) and B6129SF2 wild-type (WT), non-transgenic controls were established from breeders purchased from the Jackson Laboratories (Bar Harbor, ME, USA). 3xTg-AD breeders were obtained in September 2014 and WT breeders were obtained in March 2015. Tissues were harvested at 6 months of age, a time point that coincides with MCI-like behavior in 3xTg-AD males [17], cortical pathology [21] and sex-dependent performance deficits [19, 20]. Tissues from 67 mice were analyzed: 3xTg-AD females ($n = 18$), 3xTg-AD males ($n = 25$), WT females ($n = 15$) and WT males ($n = 9$). Mice were housed in groups of 2-4 mice/cage and maintained under standard laboratory conditions. All mice were kept in polypropylene cages (7 1/2" x 11 1/2" x 5", Ancare Corp., Bellmore, NY, USA) covered with micro-filter tops (Ancare Corp.) under reversed lighting conditions (light from 7 P.M.-7 A.M.), room temperature ~22°C, humidity ~62%, low fat rodent chow (Teklad 22/5 rodent diet, Envigo, Somerset, NJ, USA), tap water available *ad libitum*, and Beta Chip bedding changed twice per week. All experimental protocols were performed in compliance with the local Animal Care Committee and the Canadian Council on Animal Care.

2.2. Hematocrit assessment

Retro-orbital blood samples were collected in heparinized Fisher microhematocrit capillary tubes prior to sacrifice. Sealed tubes were centrifuged for 10 min and read in a Critocaps reader as described previously [17].

2.3. Tissue collection

Six-month-old mice were killed with ketamine/xylazine and tissues were harvested as previously described [17]. Whole blood was collected from the peritoneal cavity within 15 sec of

severing the inferior vena cava. Following centrifugation (5 min at $10,000 \times g$, Eppendorf MiniSpin Plus; Fisher Scientific Canada, Ottawa, ON, Canada), serum was collected and stored at -20°C for quantification of autoantibodies. Extracted organs were weighed immediately using an analytical balance (Mettler Toledo AB54-S; VWR Scientific of Canada, Mississauga, ON, Canada). Wet spleen mass was recorded as a measure of splenomegaly, a reliable indicator of systemic autoimmunity in diseased mice [22]. Spleens were wet weighed, collected in cold phosphate-buffered saline (PBS), kept on ice and then processed for flow cytometry analysis of T-splenocyte distribution. Brains were wet weighed before removing cortical hemispheres which were flash frozen in liquid nitrogen and stored at -80°C for further processing.

2.4. Anti-nuclear antibody (ANA) immunofluorescence assay

The ANA test was performed in a fully-automated slide processor (IF Sprinter). Serum samples were diluted 1:50 in sample buffer (pH 7.2), and 30 μl of the diluted serum was pipetted onto HEp-2 cell slides (EUROIMMUN Canada, Mississauga, ON). Slides were incubated for 30 min at room temperature and washed four times with phosphate-buffered saline solution containing 0.2% Tween-20 (PBS-T). Thirty microliters of 1:100 diluted rabbit anti-mouse IgG-fluorescein isothiocyanate (FITC) conjugate (Sigma-Aldrich, Oakville, ON, Canada) were pipetted into each well. The slides were washed again as above after 30 min incubation with the conjugate. Ten microliters of mounting medium were added to each well and the slide was sealed with a cover glass. Results were obtained by viewing slides under an LED-fluorescence microscope (EUROStar III).

2.5. Anti-double-stranded DNA (anti-dsDNA) enzyme-linked immunosorbent assay

Anti-dsDNA autoantibodies in serum were quantified in a fully-automated ELISA analyzer (EUROIMMUN Analyzer I). Briefly, 100 μ l of each serum sample (1:200 dilution in sample buffer) were transferred into the corresponding microtiter plate well coated with antigen substrate of dsDNA complexed with nucleosomes and coupled to the solid phase (EUROIMMUN pre-coated microtiter plate). Samples were incubated for 30 min at room temperature and then washed three times with 450 μ l of working strength wash buffer (EUROIMMUN). One hundred microliters of 1:2000 diluted rabbit anti-mouse IgG-horseradish peroxidase (HRP) conjugate (Promega, Madison, WI, USA) were added to microtiter plate wells and left to incubate for 30 min. The plate was washed to remove unbound HRP enzyme conjugate, and 100 μ l of 3,3',5,5'-tetramethylbenzidine enzyme/substrate solution was pipetted into each well and incubated for 20 min at room temperature. One hundred microliters of stop solution (EUROIMMUN) were added to each well, and the microtiter plate was shaken for 5 sec at 20 Hz. Optical density was determined at a wavelength of 450 nm and a reference wavelength of 620 nm. Results are expressed as relative optical densities.

2.6. Flow cytometry analysis of T-cells in spleen

Splenocyte single cell suspensions were prepared as described earlier [17] and stained for T-cell surface markers: APC-anti-CD3 (BD Pharmingen, San Diego, CA, USA), FITC-anti-CD4, and PE-anti-CD8 (eBiosciences, San Diego, CA, USA). Data were acquired with a BD FACSCanto (Becton Dickinson, Mississauga, ON) flow cytometer and analyzed using FlowJo software (TreeStar, Ashland, OR, USA). Compensation controls were set up with single staining for each of the antibodies, including a negative control, using BD CompBeads (BD Biosciences, San Diego, CA, USA). Debris were excluded, and lymphocytes included, using a forward scatter

area (FSC-A) versus side scatter area (SSC-A) gate. Single cells (singlets) were then selected on a FSC-A versus FSC-W plot. For each sample, 100,000 events were acquired.

2.7. Protein extraction

Extraction of soluble tau and A β species were based on published methods [23]. In brief, cortical samples (approx. 100 mg) were sonicated in tris-buffered saline (TBS) with protease (cOmpleteTM ULTRA Tablets, Mini, EASYpack Protease Inhibitor Cocktail) and phosphatase (PhosSTOPTM EASYpack, Phosphatase Inhibitor Tablets) inhibitors (Roche, Mississauga, ON). The samples were then kept on ice for 10 min, followed by centrifugation for 10 min at 14 000 \times g at 4°C. Supernatants were collected, aliquoted and frozen at -80°C for subsequent analysis. Protein concentration was measured using a detergent-compatible (DC) protein assay (Bio-Rad Laboratories, Mississauga, ON).

2.8. Western blotting for soluble tau and phospho-tau

Twelve percent sodium dodecyl sulfate-polyacrylamide gels were used to separate 20 μ g of total protein under reducing conditions before transferring to polyvinylidene fluoride (PVDF) membranes (Immobilon, Millipore, MA, USA). Transfer was followed by membrane blocking with a 1:1 solution of PBS (pH 7.4) and Odyssey Blocking Buffer (Cedarlane, Burlington, ON, Canada) for one hour at room temperature. After blocking, membranes were probed overnight at 4°C using mouse monoclonal 39E10 (total tau; Covance, Princeton, NJ, USA; diluted 1:2000), rabbit monoclonal phospho-tau Thr181 (1:1000 dilution; Cell Signaling Technology, Danvers, MA, USA) and rabbit monoclonal phospho-tau Ser202 (1:1000 dilution; Cell Signaling Technology). Samples were normalized using mouse β -actin monoclonal antibody (BioLegend,

San Diego, CA, USA; dilution 1:10 000). Probing was followed by washes using PBS containing 0.5% Tween-20. Membranes were then incubated with secondary antibodies IRDye 680-conjugated goat anti-rabbit and IRDye 800CW-conjugated goat anti-mouse (LI-COR Biosciences, Lincoln, NE, USA; diluted 1:8000) for one hour at room temperature, washed with 0.1% PBS-T, and scanned using an Odyssey Infrared Imaging System (LI-COR Biosciences, Lincoln, NE, USA). Samples were run in duplicate, and band intensities were quantified by densitometry with local background subtraction using LI-COR Odyssey Software, version 2.0.

2.9. *A β ELISA*

Levels of A β ₄₂ and A β ₄₀ in the TBS-soluble fraction were assayed using Colorimetric BetaMark β -Amyloid x-42 or x-40 ELISA kits per manufacturer's instructions (Biolegend, San Diego, CA, USA). A β ₄₂ and A β ₄₀ concentrations were acquired with a MultiskanGO and SkanIt software (Thermo Scientific, Nepean, ON, Canada) at 620 nm. Values are presented as pg β -amyloid per mg of total protein.

2.10. *Quantitative reverse transcription polymerase chain reaction (qRT-PCR)*

Frozen cortical tissue from transgenic mice was sonicated (Sonic Dismembrator Model 100, Fisher Scientific) in a 1:10 w/v ratio in Trizol® (Invitrogen, Burlington, ON). Sonicates were centrifuged and RNA was extracted using Invitrogen's protocol through the collection of the RNA-containing aqueous phase. The RNA was further purified and DNase treated using an RNeasy® Mini Kit (Qiagen, Mississauga, ON) according to the manufacturer's instructions. RNA concentration and purity were determined by Multiskan GO and SkanIT software at 260/280 nm. RNA integrity was visualized by agarose gel electrophoresis.

One microgram of each RNA sample was reverse transcribed in a 20 μ l reaction using Superscript III[®] (Invitrogen) following the manufacturer's protocol. Negative controls lacking reverse transcriptase were included to confirm lack of genomic DNA contamination. Each 20 μ l real-time PCR reaction contained 300 nM each forward and reverse BDNF primers [GenBank: NM_001048139.1] (forward 5'-GCG GCA GAT AAA AAG ACT GC-3', reverse 5'-CTT ATG AAT CGC CAG CCA AT-3', Mobix, Hamilton, ON, Canada) or β -actin primers [GenBank: NM_007393.5], forward 5'-AGC CAT GTA CGT AGC CAT CC-3', reverse 5'-CTC TCA GCT GTG GTG GTG AA-3'), 10 μ l of SYBR[®] Green qPCR SuperMix UDG (Invitrogen), 30 nM of reference dye ROX (Invitrogen) and 1 μ l cDNA. Standards for absolute quantification of BDNF were PCR products generated using target-specific primers. PCR products were gel purified using a Qiagen kit and quantified by spectrophotometry (Thermo Scientific NanoDrop 2000c; Fisher Scientific, Toronto, ON, Canada). Standards for β -actin were generated from a commercially available plasmid (Invitrogen). Real-time amplifications were carried out in triplicate using the MX3000P PCR system (Stratagene, La Jolla, CA, USA) and the following thermal profile: 2 min at 50°C, 2 min at 95°C followed by 40 cycles of 95°C for 30 s, 58°C for 30 s, and 72°C for 45 s for BDNF. The thermal profile for β -actin was: 95°C for 15 s, 58°C for 30 s, and 72°C for 30 s. Standard curve R^2 values were > 0.995 and efficiencies were $> 90\%$. Following 40 cycles of amplification, a dissociation curve was added to determine if any secondary products had formed. mRNA copy numbers of BDNF are presented as a ratio to copy numbers of the housekeeping gene β -actin, which did not vary between groups.

Expression of two H2A variants, macroH2A and H2A.X were analyzed by qRT-PCR, performed as described previously [24]. Genes of interest were normalized against the geometric mean of Gapdh and HPRT, and relative enrichment was normalized to WT females. Forward and

reverse primers used were as follows: H2afy [GenBank: NM_001159513.1], 5'-CCC GGA AGT CTA AGA AGC AGG G-3' and 5'-AGG ATT GAT TAT GGC CTC CAC C-3'; H2afy2 [GenBank: NM_207000.2], 5'-CGT TCC CCA GTG GCA GAA ACT-3' and 5'-CCT GCA CGT AGA TGC CGA T-3'; H2afx [GenBank: NM_010436.2], 5'-TCG CAG GCC TCT CAG GAG TA-3' and 5'-CGA AGT GGC TCA GCT CTT TCT- 3'; Gapdh [GenBank: NM_001289726.1], 5'-GTG GAG TCA TAC TGG AAC ATG TAG-3' and 5'-AAT GGT GAA GGT CGG TGT G-3'; HPRT [GenBank: NM_013556.2] 5'-GGA GTC CTG TTG ATG TTG CCA GTA-3' and 5'-GGG ACG CAG CAA CTG ACA TTT CTA-3'.

2.11. Statistical analysis

Statistical analyses were performed using SPSS 20 software (IBM Corp., Armonk, NY, USA). Multi- and univariate analysis of variance (ANOVA), Tukey's HSD, Kruskal-Wallis H and Mann–Whitney U tests were used for group comparisons with the criterion for statistical significance set at $p \leq .05$. Groups were treated independently for post-hoc analysis and conceptually meaningful significant differences are marked on the graphs with mean values \pm SEM ($p \leq .05$, $p < .01$ and $p < .001$ are shown as *, **, and ***, respectively).

3. Results

3.1. Body and organ weights

Six-month-old WT females weighed less than age-matched WT males, but this sex discrepancy was not detected in the 3xTg-AD group (Genotype \times Sex: $F_{1,63} = 4.156$, $p = 0.046$; WT Males vs WT Females: Tukey's HSD = 6.651, $p = 0.008$, **Figure 1A**). 3xTg-AD males and

females also exhibited comparable brain weight, which was lower than in sex-matched WT controls (Genotype: $F_{1,62} = 32.951$, $p < 0.001$, **Figure 1B**). Spleen enlargement was more profound in 3xTg-AD males than in females of the same strain (Genotype \times Sex: $F_{1,63} = 6.647$, $p = 0.012$; 3xTg Males vs 3xTg Females: Tukey's HSD = 303.1, $p < 0.001$, **Figure 1C**). These findings suggest that lower brain mass in 3xTg-AD mice is not associated with lower body mass, yet coincides with strain- and sex-specific splenomegaly.

3.2. *T-lymphocyte phenotypes*

The loss of CD4/CD8 markers and the emergence of “double-negative” clones of T-cells are well-established phenomena in many systemic autoimmune diseases [25, 26]. Considering that the spleen is a major source of immune cells [27], we investigated whether 3xTg-AD males and females exhibit sex-dependent alterations in splenic T-cell populations. Representative dot plots of spleen-derived CD3⁺ (top), CD3⁺CD8⁺ (middle), CD3⁺CD4⁺ cells (bottom) from individual mice in each group are shown in **Figure 2A**. Quantitative assessment of means from each group revealed that T-lymphocyte populations were not equal across the groups (Genotype \times Sex: Wilk's $\Lambda = 0.511$, $F_{3,12} = 3.825$, $p = 0.039$). Further analysis of subpopulations revealed that 3xTg-AD males showed more pronounced reduction in cells expressing CD3 (Genotype \times Sex: $F_{1,15} = 10.424$, $p = 0.006$; 3xTg Males vs 3xTg Females: Tukey's HSD = 9.203, $p = 0.004$, **Figure 2B**) and CD3/CD8 markers (Genotype \times Sex: $F_{1,15} = 5.324$, $p = 0.036$; 3xTg Males vs 3xTg Females: Tukey's HSD = 5.622, $p = 0.002$, **Figure 2C**). However, this interaction did not reach statistical significance with the current sample size, but merely revealed an overall reduction in CD3⁺CD4⁺ cells in 3xTg-AD mice (Genotype: $F_{1,15} = 54.163$, $p < 0.001$, **Figure 2D**). Thus, the

3xTg-AD strain in general, and males in particular, develop a significant reduction in spleen-derived CD⁺ clones by 6 months of age.

3.3. Serological measures

Although 6-month old females from both groups were mostly negative for ANA staining, serum samples from 3xTg-AD and WT males showed ANA positivity to differing degrees (Chi-Square test $p < 0.01$, $\chi^2 = 12.060$, $df = 3$, **Figure 3A**). 3xTg-AD males exhibited either homogenous (4/5), or spindle fiber (1/5) staining patterns, while sex-matched WT controls (2/3) displayed weaker staining of nucleoli. Quantification of anti-dsDNA antibodies by ELISA revealed significant differences across groups, with 3xTg-AD males having higher levels than females ($H = 10.425$, $df = 3$, $p = 0.015$; 3xTg Males vs 3xTg Females: Mann-Whitney $U = 15$, $p = 0.049$, **Figure 3B**) or WT controls. The elevation in serum autoantibodies coincided with lower hematocrit in 3xTg-AD males than in 3xTg-AD females ($H = 12.352$, $df = 3$, $p = 0.006$; 3xTg Males vs 3xTg Females: Mann-Whitney $U = 15$, $p = 0.0014$, **Figure 3C**), suggesting the early development of autoimmune hemolytic anemia, as observed previously in some 1-year-old males [17]. Considering that the severity of splenomegaly and the reduction of T-lymphocytes are also more profound in 3xTg-AD males than in females, these results suggest sex is an important factor in determining the magnitude of immunological perturbations.

3.4. Tau, A β , and BDNF

Although sex differences were originally described in plaque-bearing 3xTg-AD mice [21], there is a growing consensus that neuronal dysfunction in AD is triggered by soluble species, rather

than insoluble tangles and plaques [28, 29]. Cortex was selected as the primary tissue of interest, as it is the site of initial intracellular and extracellular neuropathology in 3xTg-AD mice [10, 21]. Representative western blots assessing TBS-soluble total tau and phosphorylated tau levels in the cortex of 6-month-old mice are shown in **Figure 4A**. With the current sample size, densitometric analysis revealed comparable total tau protein levels between 3xTg-AD and WT mice at this time point (Genotype: $F_{1,9} = 1.164$, n.s., **Figure 4B**). TBS-soluble phospho-tau levels were also similar between all groups for both Thr181 (Genotype: $F_{1,9} = 0.464$, n.s., **Figure 4C**) and Ser202 (Genotype: $F_{1,9} = 0.638$, n.s., **Figure 4D**) phosphorylation sites. Conversely, A β_{40} levels in TBS-soluble fractions were elevated in the cortex of 3xTg-AD mice in comparison to WT controls (325 pg/mg tissue vs 200 pg/mg tissue), irrespective of sex (Genotype: $F_{1,30} = 16.421$, $p < 0.001$, **Figure 4E**). A β_{42} levels were similarly raised in 6-month-old 3xTg-AD mice (Genotype: $F_{1,30} = 41.994$, $p < 0.001$, **Figure 4F**). However, there were no differences in A β_{42} levels between 6-month-old 3xTg-AD males and females and no genotype effects when the ratio of A β_{42} /A β_{40} was calculated (data not shown).

Tau [30] and A β species [31, 32] may exert their neurotoxic effects at least in part by downregulating BDNF, which is crucial for synaptic plasticity and for memory consolidation [33]. Given the essential role of BDNF downregulation in AD [34-36] and its regulation by histone modifications [37], we investigated whether 3xTg-AD mice exhibit soluble tau- and A β -associated declines in BDNF expression. BDNF mRNA was significantly downregulated in 3xTg-AD mice compared to WT (Genotype: $F_{1,36} = 6.213$, $p < 0.05$, **Figure 4G**), without affecting one sex more than the other. Collectively, the results suggest that by 6 months of age and independent of sex, increased production of soluble A β species is associated with downregulation of BDNF expression in the cortex of 3xTg-AD mice.

3.5. Expression of histone H2A variants

Histone variants, which replace canonical histones in nucleosomes, were recently implicated in neural plasticity [24, 38, 39] and neurodegeneration [40-42], but their roles in AD have not been studied. Recent evidence suggests that transcriptional regulation of histone variant expression by stable and transient environmental conditions is functionally relevant [24, 38, 39], prompting us to investigate their expression levels as an initial step in evaluating a potential novel role of histone variants in AD. The expression of *H2afy*, which encodes the histone variant macroH2A.1, was lower in WT males compared to WT females, whereas sex differences were not found for 3xTg-AD mice (Genotype \times Sex: $F_{1,16} = 4.8$, $p = 0.04$; WT Males vs WT Females, $p < 0.05$; 3xTg Males vs WT Males, $p < 0.05$, **Figure 5A**). Moreover, *H2afy* levels were higher in 3xTg-AD males compared to WT males. In contrast, no sex or genotype differences were observed in the expression of *H2afy2*, which codes for the histone variant macroH2A.2 (**Figure 5B**). The histone variant H2A.X, encoded by *H2afx*, was increased in 3xTg-AD mice compared to WT controls, irrespective of sex (Genotype: $F_{1,15} = 10.15$, $p = 0.006$; **Figure 5C**). Taken together, these findings suggest that genes encoding variants of the canonical histone H2A are altered in a histone-specific manner in the 3xTg-AD model. In contrast to WT, where histone H2A variants differ in a sex-specific manner, in 3xTg-AD mice there are no such sex differences.

4. Discussion

The present study aimed to compare the immune status, soluble AD-like pathology and expression of cortical markers implicated in learning/memory and neurodegenerative processes in male and female 3xTg-AD mice. Six-month-old 3xTg-AD mice of both sexes exhibited spleen

enlargement that was accompanied by a reduction in subpopulations of CD3⁺, CD8⁺, and CD4⁺ T-lymphocytes. The severity of the splenomegaly and the paucity of spleen-derived CD⁺ clones were more pronounced in 3xTg-AD males than in females. Similar sexual dimorphism was noted with respect to serum autoantibodies and hematocrit, suggesting autoantibody-induced hemolytic anemia in some adult 3xTg-AD males. Despite the aforementioned sex-dependent changes in immunophenotype, 3xTg-AD males and females showed comparable alterations in established AD-like markers. In particular, both sexes had smaller brains, produced similar loads of soluble A β ₄₂ and displayed similar downregulation of BDNF in comparison to age- and sex-matched WT controls. In contrast, the expression of histone variants in 3xTg-AD mice was altered in a histone-specific manner, whereas the sex-specific differences in histone variant expression seen in WT mice were not present in the 3xTg-AD mice. These results implicate epigenetic alterations in nucleosome composition as potential regulators of sex-specific outcomes. These findings demonstrate that 3xTg-AD mice exhibit an early, systemic autoimmune response prior to overt AD-like pathology and that sex is a key factor in determining the magnitude of immunological perturbations. Based on our earlier observation of the lack of AD-like pathology in one-year-old 3xTg-AD males [17] and the confirmatory claims by the donating investigator (<https://www.jax.org/strain/004807>), it is clear that the current 3xTg-AD phenotype has drifted from its original phenotype described more than 15 years ago. Therefore it is possible that the observed sex-dependent autoimmune manifestations may interfere with the deposition of plaques and tangles (**Figure 6**). The origins, timing in ontogenesis and molecular mechanisms of this sex-dependent autoimmunity require further studies.

The current results are consistent with an increasing number of observations pointing to immunological dysfunction in the 3xTg-AD substrain [17, 43-50]. However, previous reports

have focused exclusively on advanced stages of the disease [43, 44, 48, 49] or failed to address the role of sex [45, 48, 50]. Our findings of sex-dependent alterations in splenic leukocyte populations are distinct from those of Subramanian and colleagues, who reported that the expression of certain lymphoid and myeloid markers (different than the population investigated here) is affected in 5-6-month-old 3xTg-AD females, but not males [47]. In support of a sex-dependent discrepancy that favors more severe manifestations in males, it has been reported that 6-month-old 3xTg-AD males exhibit premature thymic involution (a sign of immunosenescence) in comparison to age-matched females [49]. This dissimilarity in immune status is exacerbated at later stages of the disease [43, 44], suggesting sex-specific signs of immunological dysfunction in the 3xTg-AD strain are progressive in nature [46].

The currently observed sexual dimorphism in the severity of autoimmune manifestations is consistent with recent studies revealing dissimilar progression of behavioral changes [19, 20, 51-55], neuropathology [21, 55-57] and longevity [58] between male and female 3xTg-AD mice. Although the direction and magnitude of functional differences seem to vary across testing age and procedures, ~6-month-old 3xTg-AD males perform more poorly than age-matched females in learning/memory tasks including the radial [20] and Barnes mazes [19]. Yet, the emergence of plaques and tangles in male 3xTg-AD mice currently does not occur until at least 15 months of age [59]. In the case of tau, neurofibrillary tangles are only present in a relatively small population of cells in CA1 and the subiculum by 15 months of age and are not present throughout the hippocampus until 26 months of age. While the classical phenotype of these animals is delayed by at least 9 months compared to the original report [10], they may still exhibit intraneuronal species of A β and hyperphosphorylated tau as early as 2 and 6 months of age, respectively [59]. The protracted delay in the production of A β and tau does not seem to occur in 3xTg-AD females,

which exhibit a more rapid and aggressive progression of AD-like disease [21, 55, 56]. However, our current analysis revealed that A β ₄₀ and A β ₄₂ levels in 6-month-old 3xTg-AD females were comparable to age-matched 3xTg-AD males. The lack of a sex discrepancy at this age is consistent with previous findings suggesting that 3xTg-AD females show more pronounced A β pathology during the plaque-bearing phase of the disease [21]. However, sex-dependent behavioral deficits at such an advanced stage are likely to reflect not only A β accumulation but also other epigenetic events [60, 61] and pathological changes, including tau hyperphosphorylation, glial activation, impaired long-term potentiation [10] and loss of neurotrophic support [62].

Our finding of BDNF downregulation in 3xTg-AD mice is in agreement with previous studies that point to a reduction in BDNF expression in AD [35, 36, 63], MCI [36], and the onset of AD-like disease in transgenic mice [32, 64], including 3xTg-AD males [60]. The early loss of BDNF expression in 3xTg-AD mice is associated with higher levels of soluble A β species in the absence of tau pathology, suggesting neurotrophic deficits in this strain are a consequence of A β accumulation [31, 32] or alternatively, a driver of A β pathology [65, 66]. Targeting of neurotrophic signaling pathways has therapeutic potential for treating synaptic and learning/memory deficits in older 3xTg-AD mice [62], but the beneficial effects may not depend on alterations in A β or tau pathology [62, 67]. This suggests that BDNF loss in 3xTg-AD mice is downstream of A β pathology [31] and that neither increased A β nor decreased BDNF (comparable between males and females at this time point) accounts for sex differences in behavioral performance [19, 20].

Epigenetic factors are involved in establishing and maintaining immune responses [68], and chromatin dysregulation (particularly in immune-response genes in the hippocampus) has been implicated in AD in both humans and mice [69, 70]. Although most studies have focused on DNA

methylation and post-translational modifications of histones, histone variants were recently identified as essential regulators of neural function [24, 38, 71]. MacroH2A.1, a variant of histone H2A, is upregulated in the blood and cortex of Huntington's patients and mice in relation to disease severity [40, 41], linking this variant to neurodegeneration. Consistent with these data, we found that macroH2A.1 is upregulated in 3xTg-AD mice, but only in males. Interestingly, WT females exhibit higher levels of macroH2A.1 than WT males, such that levels in WT females were comparable to the levels seen in 3xTg-AD males. H2A.X is another H2A variant that is rapidly phosphorylated in response to dsDNA breaks and plays a key role in DNA damage repair [72]. Increased levels of phosphorylated H2A.X are found in cortical and hippocampal astrocytes of AD patients [42]. Our data reveal that overall levels of H2A.X transcript are similarly increased in 3xTg-AD mice, irrespective of sex. It is unclear whether these changes occurred spontaneously (e.g. allowing for more rapid repair of accumulating double-strand breaks in AD [73]), or if they contribute to brain pathology. Taken together, these results suggest that altered availability of specific histone variant subtypes contributes to altered nucleosome composition in 3xTg-AD mice. Given that our analyses were limited to mRNA levels of these histone variants, it is not clear if changes in gene expression reflect alterations in their incorporation into chromatin. However, recent studies showed that transcriptional regulation of histone variants in the brain is associated with altered behavioral outcomes [24, 38, 39], and on this basis, our data implicate macroH2A.1 and H2A.X as novel targets for future epigenetic studies of AD. Indeed, full-scale studies investigating genome-wide chromatin binding patterns and functional implications of these histone variants are currently underway.

The nature of the sex-dependent autoimmune response in the 3xTg-AD strain prior to plaque and tangle development remains unknown. The delay of AD-like neuropathology in males

suggests that early systemic autoimmunity may constitute an immune response to systemic amyloidosis and plaque deposition. In particular, our initial study with 1-year-old males revealed both splenomegaly and hepatomegaly [17], which are common markers of amyloidosis. Indeed, immunization of 3xTg-AD mice with a DNA epitope vaccine induces high titers of anti-A β antibody, which in turn inhibits the accumulation of A β , reduces glial activation, and prevents behavioral deficits [74]. Yet, post-vaccination improvements in behavioral performance do not seem to rely exclusively on robust reduction in A β burden in the brain [75, 76]. This suggests that the accumulation of A β may not be sufficient to cause dementia but could represent a trigger to activate the immune system [77]. Although sex-specific differences in immune function in our study may be linked to sex-specific differences in behavior, our results suggest that immune-mediated reduction in A β is not the mechanism. Although the precise mechanisms underlying the beneficial effects of immunization remain unknown, studies support the role of antibody-mediated plaque clearance via microglial phagocytosis [78]. This is consistent with the delay in plaque deposition in male 3xTg-AD mice, which exhibit greater autoimmunity than females. Females may not be able to readily mount such an immune response, rendering them vulnerable to plaque accumulation at earlier ages. Currently, we do not know the origins of systemic autoimmunity or the identity of key factors accounting for the difference between the sexes in their immune status. Future experiments involving manipulations of systemic autoimmunity in pregnant dams and/or hormonal treatments in neonates may help in addressing these research questions. While the Thy1.2 promoter drives transgene expression predominantly in the CNS and expression hasn't been documented in peripheral tissues [10], further studies are required to confirm whether signs of systemic involvement are epiphenomena or consequences of transgene expression in other

organs. Although more research is needed on the origins of autoimmunity, it is clear that sex should be included as a main factor when designing future experimental and clinical studies.

Acknowledgement

This work was supported by a grant from the Canadian Institutes of Health Research (PJT-149031).

Figure Captions

Figure 1: *Body and organ weights at 6 months of age.* (A) WT females weighed significantly less than age-matched WT males and 3xTg-AD mice. (B) Post-mortem assessment of wet brain mass revealed that 3xTg-AD males and females had smaller brains than WT controls. (C) Enlargement of the spleen, a reliable indicator of autoimmunity, was more severe in 3xTg-AD males than in females. 3xTg-AD females ($n = 18$), 3xTg-AD males ($n = 25$), WT females ($n = 15$) and WT males ($n = 9$). Overall group comparisons were carried out using two-way ANOVA (sex \times genotype) followed by post-hoc Tukey's HSD test. Error bars = SEM, ** $p < 0.01$, *** $p < 0.001$.

Figure 2: *T-cell phenotypes.* Single cell suspensions of spleens from 6-month-old 3xTg-AD and WT mice were stained for APC-anti-CD3, FITC-anti-CD4, and PE-anti-CD8 and analyzed by flow cytometry. (A) Representative dot plots of triplicate experiments highlighting the gating strategy and relative percentage of cellular subsets of interest in the top and bottom right corners are shown. (B-D) Mean \pm SEM values of CD3⁺, CD3⁺CD8⁺ and CD3⁺CD4⁺ cells as a percentage of total cells are shown. Both sexes of 3xTg-AD mice displayed a significant reduction in T-cells in comparison to age- and sex-matched WT controls, but the severity of the loss of CD3⁺ and CD3⁺CD8⁺ T-cells was exacerbated in males compared to females. Overall group comparisons ($n = 3-5$ /group) were carried out using two-way ANOVA (sex \times genotype) followed by post-hoc Tukey's HSD test. Error bars = SEM, ** $p < 0.01$, *** $p < 0.001$.

Figure 3: *Serological markers of systemic autoimmunity at 6 months of age.* (A) Representative images of serum autoantibodies against cell nuclei (ANA) revealed increased ANA positivity in

3xTg-AD males (white arrows), but not females. Serum from age-matched WT males exhibited nucleoli-positive staining (white arrowheads), which was not seen in samples from WT females or 3xTg-AD males. **(B)** Despite this positivity in controls, serum levels of anti-dsDNA were particularly elevated in 3xTg-AD males in comparison to age-matched females. **(C)** Increased levels of autoantibodies in the serum of 3xTg-AD males were associated with a significant reduction in the volume percentage of red blood cells in blood. 3xTg-AD females ($n = 6-11$), 3xTg-AD males ($n = 12$), WT females ($n = 6$) and WT males ($n = 3-4$). Group comparison was carried out using Kruskal-Wallis non-parametric test followed by pair-wise Mann–Whitney U tests. Error bars = SEM, * $p < 0.05$, ** $p < 0.01$.

Figure 4: *Tau, A β , and BDNF in cortical samples from 6-month-old mice.* **(A)** Representative western blots illustrating tau, phosphorylated-tau and β -actin protein levels in TBS-soluble homogenates extracted from the cortex of 6-month-old mice. **(B-D)** Densitometric analyses of western blots (normalized to β -actin) revealed equal intensities for total tau probed with 39E10 and for tau phosphorylated at Thr181 and Ser202 sites. Samples were run in duplicate and band intensities were normalized across 2 blots. **(E-F)** TBS-soluble A β_{40} and A β_{42} were elevated in the cortex of 3xTg-AD mice compared to WT, irrespective of sex. **(G)** Downregulation of BDNF mRNA expression (normalized to β -actin) in 3xTg-AD mice compared to WT, as analyzed by qRT-PCR. Abbreviations: A β , amyloid beta; BDNF, brain-derived neurotrophic factor; mRNA, messenger RNA; pTau, phosphorylated tau; tTau, total tau; TBS, tris-buffered saline. Overall group comparisons ($n = 3-4$ /group for western blot analysis, $n = 6-10$ /group for A β ELISAs and BDNF qRT-PCR) were carried out using two-way ANOVA (sex \times genotype) followed by post-hoc Tukey's HSD test. Error bars = SEM, * $p < 0.05$, *** $p < 0.001$.

Figure 5: *Expression of histone H2A variants in cortical samples from 6-month-old mice.* (A) Compared to WT males, 3xTg-AD males exhibited increased levels of macroH2A.1. (B) The expression of *h2afy2*, which encodes the histone variant macroH2A.2, was comparable between all groups. (C) H2A.X levels were increased in 3xTg-AD mice irrespective of sex. Overall group comparisons (n = 3-9/group) were carried out using two-way ANOVA (sex x genotype) followed by post-hoc Tukey's HSD test. Error bars = SEM, *p < 0.05, **p < 0.01.

Figure 6: *Proposed network in the current 3xTg-AD model.* MCI-like behavior in 3xTg-AD mice may result from the transfer of human gene(s) that regulates the immune system in a sex-dependent manner. Enhanced systemic autoimmunity in young males may reflect an early, immune mechanism that interferes with the deposition of plaques and tangles. Given that sex clearly determines the severity of immunological perturbations, further studies are required to elucidate if sex chromosomes, sex hormones, and/or intrauterine environment drive systemic autoimmunity in the AD-like disease.

REFERENCES

- [1] Querfurth HW, LaFerla FM (2010) Alzheimer's disease. *N Engl J Med* **362**, 329-344.
- [2] Alzheimer's Association (2016) 2016 Alzheimer's disease facts and figures. *Alzheimers Dement* **12**, 459-509.
- [3] Carter CL, Resnick EM, Mallampalli M, Kalbarczyk A (2012) Sex and gender differences in Alzheimer's disease: recommendations for future research. *J Womens Health (Larchmt)* **21**, 1018-1023.
- [4] Chene G, Beiser A, Au R, Preis SR, Wolf PA, Dufouil C, Seshadri S (2015) Gender and incidence of dementia in the Framingham Heart Study from mid-adult life. *Alzheimers Dement* **11**, 310-320.
- [5] Ungar L, Altmann A, Greicius MD (2014) Apolipoprotein E, gender, and Alzheimer's disease: an overlooked, but potent and promising interaction. *Brain Imaging Behav* **8**, 262-273.
- [6] Altmann A, Tian L, Henderson VW, Greicius MD, Alzheimer's Disease Neuroimaging Initiative I (2014) Sex modifies the APOE-related risk of developing Alzheimer disease. *Ann Neurol* **75**, 563-573.
- [7] Heneka MT, Carson MJ, El Khoury J, Landreth GE, Brosseron F, Feinstein DL, Jacobs AH, Wyss-Coray T, Vitorica J, Ransohoff RM, Herrup K, Frautschy SA, Finsen B, Brown GC, Verkhratsky A, Yamanaka K, Koistinaho J, Latz E, Halle A, Petzold GC, Town T, Morgan D, Shinohara ML, Perry VH, Holmes C, Bazan NG, Brooks DJ, Hunot S, Joseph B, Deigendesch N, Garaschuk O, Boddeke E, Dinarello CA, Breitner JC, Cole GM, Golenbock DT, Kummer MP (2015) Neuroinflammation in Alzheimer's disease. *Lancet Neurol* **14**, 388-405.
- [8] Sevigny J, Chiao P, Bussiere T, Weinreb PH, Williams L, Maier M, Dunstan R, Salloway S, Chen T, Ling Y, O'Gorman J, Qian F, Arastu M, Li M, Chollate S, Brennan MS, Quintero-Monzon O, Scannevin RH, Arnold HM, Engber T, Rhodes K, Ferrero J, Hang Y, Mikulskis A, Grimm J, Hock C, Nitsch RM, Sandrock A (2016) The antibody aducanumab reduces Abeta plaques in Alzheimer's disease. *Nature* **537**, 50-56.
- [9] Bilkei-Gorzo A (2014) Genetic mouse models of brain ageing and Alzheimer's disease. *Pharmacol Ther* **142**, 244-257.
- [10] Oddo S, Caccamo A, Shepherd JD, Murphy MP, Golde TE, Kaye R, Metherate R, Mattson MP, Akbari Y, LaFerla FM (2003) Triple-transgenic model of Alzheimer's disease with plaques and tangles: intracellular Abeta and synaptic dysfunction. *Neuron* **39**, 409-421.
- [11] Billings LM, Oddo S, Green KN, McGaugh JL, LaFerla FM (2005) Intraneuronal Abeta causes the onset of early Alzheimer's disease-related cognitive deficits in transgenic mice. *Neuron* **45**, 675-688.
- [12] Oddo S, Caccamo A, Tseng B, Cheng D, Vasilevko V, Cribbs DH, LaFerla FM (2008) Blocking Abeta42 accumulation delays the onset and progression of tau pathology via the C terminus of heat shock protein70-interacting protein: a mechanistic link between Abeta and tau pathology. *J Neurosci* **28**, 12163-12175.

- [13] Tseng BP, Green KN, Chan JL, Blurton-Jones M, LaFerla FM (2008) Abeta inhibits the proteasome and enhances amyloid and tau accumulation. *Neurobiol Aging* **29**, 1607-1618.
- [14] Janelsins MC, Mastrangelo MA, Oddo S, LaFerla FM, Federoff HJ, Bowers WJ (2005) Early correlation of microglial activation with enhanced tumor necrosis factor-alpha and monocyte chemoattractant protein-1 expression specifically within the entorhinal cortex of triple transgenic Alzheimer's disease mice. *J Neuroinflammation* **2**, 23.
- [15] Kitazawa M, Oddo S, Yamasaki TR, Green KN, LaFerla FM (2005) Lipopolysaccharide-induced inflammation exacerbates tau pathology by a cyclin-dependent kinase 5-mediated pathway in a transgenic model of Alzheimer's disease. *J Neurosci* **25**, 8843-8853.
- [16] Sy M, Kitazawa M, Medeiros R, Whitman L, Cheng D, Lane TE, Laferla FM (2011) Inflammation induced by infection potentiates tau pathological features in transgenic mice. *Am J Pathol* **178**, 2811-2822.
- [17] Marchese M, Cowan D, Head E, Ma D, Karimi K, Ashthorpe V, Kapadia M, Zhao H, Davis P, Sakic B (2014) Autoimmune manifestations in the 3xTg-AD model of Alzheimer's disease. *J Alzheimers Dis* **39**, 191-210.
- [18] Cho SM, Lee S, Yang SH, Kim HY, Lee MJ, Kim HV, Kim J, Baek S, Yun J, Kim D, Kim YK, Cho Y, Woo J, Kim TS, Kim Y (2016) Age-dependent inverse correlations in CSF and plasma amyloid-beta(1-42) concentrations prior to amyloid plaque deposition in the brain of 3xTg-AD mice. *Sci Rep* **6**, 20185.
- [19] Stover KR, Campbell MA, Van Winssen CM, Brown RE (2015) Early detection of cognitive deficits in the 3xTg-AD mouse model of Alzheimer's disease. *Behav Brain Res* **289**, 29-38.
- [20] Stevens LM, Brown RE (2015) Reference and working memory deficits in the 3xTg-AD mouse between 2 and 15-months of age: a cross-sectional study. *Behav Brain Res* **278**, 496-505.
- [21] Hirata-Fukae C, Li HF, Hoe HS, Gray AJ, Minami SS, Hamada K, Niikura T, Hua F, Tsukagoshi-Nagai H, Horikoshi-Sakuraba Y, Mughal M, Rebeck GW, LaFerla FM, Mattson MP, Iwata N, Saido TC, Klein WL, Duff KE, Aisen PS, Matsuoka Y (2008) Females exhibit more extensive amyloid, but not tau, pathology in an Alzheimer transgenic model. *Brain Res* **1216**, 92-103.
- [22] Theofilopoulos AN (1992) Murine models of lupus In *Systemic lupus erythematosus*, Lahita RG, ed. Churchill Livingstone, New York, pp. 121-194.
- [23] Michalski B, Corrada MM, Kawas CH, Fahnestock M (2015) Brain-derived neurotrophic factor and TrkB expression in the "oldest-old," the 90+ Study: correlation with cognitive status and levels of soluble amyloid-beta. *Neurobiol Aging* **36**, 3130-3139.
- [24] Zovkic IB, Paulukaitis BS, Day JJ, Etikala DM, Sweatt JD (2014) Histone H2A.Z subunit exchange controls consolidation of recent and remote memory. *Nature* **515**, 582-586.
- [25] Thomson CW, Lee BP, Zhang L (2006) Double-negative regulatory T cells: non-conventional regulators. *Immunol Res* **35**, 163-178.
- [26] Strober S, Cheng L, Zeng D, Palathumpat R, Dejbakhsh-Jones S, Huie P, Sibley R (1996) Double negative (CD4-CD8- alpha beta+) T cells which promote tolerance induction and regulate autoimmunity. *Immunol Rev* **149**, 217-230.
- [27] Mebius RE, Kraal G (2005) Structure and function of the spleen. *Nat Rev Immunol* **5**, 606-616.

- [28] Haass C, Selkoe DJ (2007) Soluble protein oligomers in neurodegeneration: lessons from the Alzheimer's amyloid beta-peptide. *Nat Rev Mol Cell Biol* **8**, 101-112.
- [29] Ferreira ST, Lourenco MV, Oliveira MM, De Felice FG (2015) Soluble amyloid-beta oligomers as synaptotoxins leading to cognitive impairment in Alzheimer's disease. *Front Cell Neurosci* **9**, 191.
- [30] Rosa E, Mahendram S, Ke YD, Ittner LM, Ginsberg SD, Fahnstock M (2016) Tau downregulates BDNF expression in animal and cellular models of Alzheimer's disease. *Neurobiol Aging* **48**, 135-142.
- [31] Garzon DJ, Fahnstock M (2007) Oligomeric amyloid decreases basal levels of brain-derived neurotrophic factor (BDNF) mRNA via specific downregulation of BDNF transcripts IV and V in differentiated human neuroblastoma cells. *J Neurosci* **27**, 2628-2635.
- [32] Peng S, Garzon DJ, Marchese M, Klein W, Ginsberg SD, Francis BM, Mount HT, Mufson EJ, Salehi A, Fahnstock M (2009) Decreased brain-derived neurotrophic factor depends on amyloid aggregation state in transgenic mouse models of Alzheimer's disease. *J Neurosci* **29**, 9321-9329.
- [33] Fahnstock M (2011) Brain-derived neurotrophic factor: the link between amyloid- β and memory loss. *Future Neurol* **6**, 627-639.
- [34] Garzon D, Yu G, Fahnstock M (2002) A new brain-derived neurotrophic factor transcript and decrease in brain-derived neurotrophic factor transcripts 1, 2 and 3 in Alzheimer's disease parietal cortex. *J Neurochem* **82**, 1058-1064.
- [35] Holsinger RM, Schnarr J, Henry P, Castelo VT, Fahnstock M (2000) Quantitation of BDNF mRNA in human parietal cortex by competitive reverse transcription-polymerase chain reaction: decreased levels in Alzheimer's disease. *Brain Res Mol Brain Res* **76**, 347-354.
- [36] Peng S, Wu J, Mufson EJ, Fahnstock M (2005) Precursor form of brain-derived neurotrophic factor and mature brain-derived neurotrophic factor are decreased in the pre-clinical stages of Alzheimer's disease. *J Neurochem* **93**, 1412-1421.
- [37] Lubin FD, Roth TL, Sweatt JD (2008) Epigenetic regulation of BDNF gene transcription in the consolidation of fear memory. *J Neurosci* **28**, 10576-10586.
- [38] Maze I, Wenderski W, Noh KM, Bagot RC, Tzavaras N, Purushothaman I, Elsasser SJ, Guo Y, Ionete C, Hurd YL, Tamminga CA, Halene T, Farrelly L, Soshnev AA, Wen D, Raffi S, Birtwistle MR, Akbarian S, Buchholz BA, Blitzer RD, Nestler EJ, Yuan ZF, Garcia BA, Shen L, Molina H, Allis CD (2015) Critical Role of Histone Turnover in Neuronal Transcription and Plasticity. *Neuron* **87**, 77-94.
- [39] Lepack AE, Bagot RC, Pena CJ, Loh YE, Farrelly LA, Lu Y, Powell SK, Lorsch ZS, Issler O, Cates HM, Tamminga CA, Molina H, Shen L, Nestler EJ, Allis CD, Maze I (2016) Aberrant H3.3 dynamics in NAc promote vulnerability to depressive-like behavior. *Proc Natl Acad Sci U S A* **113**, 12562-12567.
- [40] Ehrlich ME, Gandy S (2011) Chromatin plasticity and the pathogenesis of Huntington disease. *Proc Natl Acad Sci U S A* **108**, 16867-16868.
- [41] Hu Y, Chopra V, Chopra R, Locascio JJ, Liao Z, Ding H, Zheng B, Matson WR, Ferrante RJ, Rosas HD, Hersch SM, Scherzer CR (2011) Transcriptional modulator H2A histone family, member Y (H2AFY) marks Huntington disease activity in man and mouse. *Proc Natl Acad Sci U S A* **108**, 17141-17146.

- [42] Myung NH, Zhu X, Kruman, II, Castellani RJ, Petersen RB, Siedlak SL, Perry G, Smith MA, Lee HG (2008) Evidence of DNA damage in Alzheimer disease: phosphorylation of histone H2AX in astrocytes. *Age (Dordr)* **30**, 209-215.
- [43] Arranz L, De Castro NM, Baeza I, Gimenez-Llort L, De la Fuente M (2011) Effect of environmental enrichment on the immunoendocrine aging of male and female triple-transgenic 3xTg-AD mice for Alzheimer's disease. *J Alzheimers Dis* **25**, 727-737.
- [44] Gimenez-Llort L, Arranz L, Mate I, De la Fuente M (2008) Gender-specific neuroimmunoendocrine aging in a triple-transgenic 3xTg-AD mouse model for Alzheimer's disease and its relation with longevity. *Neuroimmunomodulation* **15**, 331-343.
- [45] Montacute R, Foley K, Forman R, Else KJ, Cruickshank SM, Allan SM (2017) Enhanced susceptibility of triple transgenic Alzheimer's disease (3xTg-AD) mice to acute infection. *J Neuroinflammation* **14**, 50.
- [46] Gimenez-Llort L, Mate I, Manassra R, Vida C, De la Fuente M (2012) Peripheral immune system and neuroimmune communication impairment in a mouse model of Alzheimer's disease. *Ann N Y Acad Sci* **1262**, 74-84.
- [47] Subramanian S, Ayala P, Wadsworth TL, Harris CJ, Vandembark AA, Quinn JF, Offner H (2010) CCR6: a biomarker for Alzheimer's-like disease in a triple transgenic mouse model. *J Alzheimers Dis* **22**, 619-629.
- [48] Yang SH, Kim J, Lee MJ, Kim Y (2015) Abnormalities of plasma cytokines and spleen in senile APP/PS1/Tau transgenic mouse model. *Sci Rep* **5**, 15703.
- [49] Gimenez-Llort L, Garcia Y, Buccieri K, Revilla S, Sunol C, Cristofol R, Sanfeliu C (2010) Gender-Specific Neuroimmunoendocrine Response to Treadmill Exercise in 3xTg-AD Mice. *Int J Alzheimers Dis* **2010**, 128354.
- [50] Haskins M, Jones TE, Lu Q, Bareiss SK (2016) Early alterations in blood and brain RANTES and MCP-1 expression and the effect of exercise frequency in the 3xTg-AD mouse model of Alzheimer's disease. *Neurosci Lett* **610**, 165-170.
- [51] Clinton LK, Billings LM, Green KN, Caccamo A, Ngo J, Oddo S, McLaugh JL, LaFerla FM (2007) Age-dependent sexual dimorphism in cognition and stress response in the 3xTg-AD mice. *Neurobiol Dis* **28**, 76-82.
- [52] Roddick KM, Roberts AD, Schellinck HM, Brown RE (2016) Sex and Genotype Differences in Odor Detection in the 3xTg-AD and 5XFAD Mouse Models of Alzheimer's Disease at 6 Months of Age. *Chem Senses* **41**, 433-440.
- [53] Blazquez G, Canete T, Tobena A, Gimenez-Llort L, Fernandez-Teruel A (2014) Cognitive and emotional profiles of aged Alzheimer's disease (3xTgAD) mice: effects of environmental enrichment and sexual dimorphism. *Behav Brain Res* **268**, 185-201.
- [54] Pietropaolo S, Sun Y, Li R, Brana C, Feldon J, Yee BK (2008) The impact of voluntary exercise on mental health in rodents: a neuroplasticity perspective. *Behav Brain Res* **192**, 42-60.
- [55] Pietropaolo S, Sun Y, Li R, Brana C, Feldon J, Yee BK (2009) Limited impact of social isolation on Alzheimer-like symptoms in a triple transgenic mouse model. *Behav Neurosci* **123**, 181-195.
- [56] Carroll JC, Rosario ER, Kreimer S, Villamagna A, Gentschein E, Stanczyk FZ, Pike CJ (2010) Sex differences in beta-amyloid accumulation in 3xTg-AD mice: role of neonatal sex steroid hormone exposure. *Brain Res* **1366**, 233-245.

- [57] Perez SE, He B, Muhammad N, Oh KJ, Fahnstock M, Ikonovic MD, Mufson EJ (2011) Cholinergic basal forebrain system alterations in 3xTg-AD transgenic mice. *Neurobiol Dis* **41**, 338-352.
- [58] Rae EA, Brown RE (2015) The problem of genotype and sex differences in life expectancy in transgenic AD mice. *Neurosci Biobehav Rev* **57**, 238-251.
- [59] Mastrangelo MA, Bowers WJ (2008) Detailed immunohistochemical characterization of temporal and spatial progression of Alzheimer's disease-related pathologies in male triple-transgenic mice. *BMC Neurosci* **9**, 81.
- [60] Walker MP, LaFerla FM, Oddo SS, Brewer GJ (2013) Reversible epigenetic histone modifications and Bdnf expression in neurons with aging and from a mouse model of Alzheimer's disease. *Age (Dordr)* **35**, 519-531.
- [61] Marques SC, Lemos R, Ferreira E, Martins M, de Mendonca A, Santana I, Outeiro TF, Pereira CM (2012) Epigenetic regulation of BACE1 in Alzheimer's disease patients and in transgenic mice. *Neuroscience* **220**, 256-266.
- [62] Blurton-Jones M, Kitazawa M, Martinez-Coria H, Castello NA, Muller FJ, Loring JF, Yamasaki TR, Poon WW, Green KN, LaFerla FM (2009) Neural stem cells improve cognition via BDNF in a transgenic model of Alzheimer disease. *Proc Natl Acad Sci U S A* **106**, 13594-13599.
- [63] Connor B, Young D, Yan Q, Faull RL, Synek B, Dragunow M (1997) Brain-derived neurotrophic factor is reduced in Alzheimer's disease. *Brain Res Mol Brain Res* **49**, 71-81.
- [64] Francis BM, Kim J, Barakat ME, Fraenkl S, Yucel YH, Peng S, Michalski B, Fahnstock M, McLaurin J, Mount HT (2012) Object recognition memory and BDNF expression are reduced in young TgCRND8 mice. *Neurobiol Aging* **33**, 555-563.
- [65] Arancibia S, Silhol M, Moulriere F, Meffre J, Hollinger I, Maurice T, Tapia-Arancibia L (2008) Protective effect of BDNF against beta-amyloid induced neurotoxicity in vitro and in vivo in rats. *Neurobiol Dis* **31**, 316-326.
- [66] Matrone C, Ciotti MT, Mercanti D, Marolda R, Calissano P (2008) NGF and BDNF signaling control amyloidogenic route and A β production in hippocampal neurons. *Proc Natl Acad Sci U S A* **105**, 13139-13144.
- [67] Castello NA, Green KN, LaFerla FM (2012) Genetic knockdown of brain-derived neurotrophic factor in 3xTg-AD mice does not alter A β or tau pathology. *PLoS One* **7**, e39566.
- [68] Mehta S, Jeffrey KL (2015) Beyond receptors and signaling: epigenetic factors in the regulation of innate immunity. *Immunol Cell Biol* **93**, 233-244.
- [69] Gjoneska E, Pfenning AR, Mathys H, Quon G, Kundaje A, Tsai LH, Kellis M (2015) Conserved epigenomic signals in mice and humans reveal immune basis of Alzheimer's disease. *Nature* **518**, 365-369.
- [70] Klein HU, Bennett DA, De Jager PL (2016) The epigenome in Alzheimer's disease: current state and approaches for a new path to gene discovery and understanding disease mechanism. *Acta Neuropathol* **132**, 503-514.
- [71] Zovkic IB, Sweatt JD (2015) Memory-Associated Dynamic Regulation of the "Stable" Core of the Chromatin Particle. *Neuron* **87**, 1-4.
- [72] Podhorecka M, Skladanowski A, Bozko P (2010) H2AX Phosphorylation: Its Role in DNA Damage Response and Cancer Therapy. *J Nucleic Acids* **2010**.

- [73] Merlo D, Mollinari C, Racaniello M, Garaci E, Cardinale A (2016) DNA Double Strand Breaks: A Common Theme in Neurodegenerative Diseases. *Curr Alzheimer Res* **13**, 1208-1218.
- [74] Movsesyan N, Ghochikyan A, Mkrtichyan M, Petrushina I, Davtyan H, Olkhanud PB, Head E, Biragyn A, Cribbs DH, Agadjanyan MG (2008) Reducing AD-like pathology in 3xTg-AD mouse model by DNA epitope vaccine - a novel immunotherapeutic strategy. *PLoS One* **3**, e2124.
- [75] Morgan D, Diamond DM, Gottschall PE, Ugen KE, Dickey C, Hardy J, Duff K, Jantzen P, DiCarlo G, Wilcock D, Connor K, Hatcher J, Hope C, Gordon M, Arendash GW (2000) A beta peptide vaccination prevents memory loss in an animal model of Alzheimer's disease. *Nature* **408**, 982-985.
- [76] Dodart JC, Bales KR, Gannon KS, Greene SJ, DeMattos RB, Mathis C, DeLong CA, Wu S, Wu X, Holtzman DM, Paul SM (2002) Immunization reverses memory deficits without reducing brain Abeta burden in Alzheimer's disease model. *Nat Neurosci* **5**, 452-457.
- [77] Kumar DK, Choi SH, Washicosky KJ, Eimer WA, Tucker S, Ghofrani J, Lefkowitz A, McColl G, Goldstein LE, Tanzi RE, Moir RD (2016) Amyloid-beta peptide protects against microbial infection in mouse and worm models of Alzheimer's disease. *Sci Transl Med* **8**, 340ra372.
- [78] Morgan D (2009) The role of microglia in antibody-mediated clearance of amyloid-beta from the brain. *CNS Neurol Disord Drug Targets* **8**, 7-15.

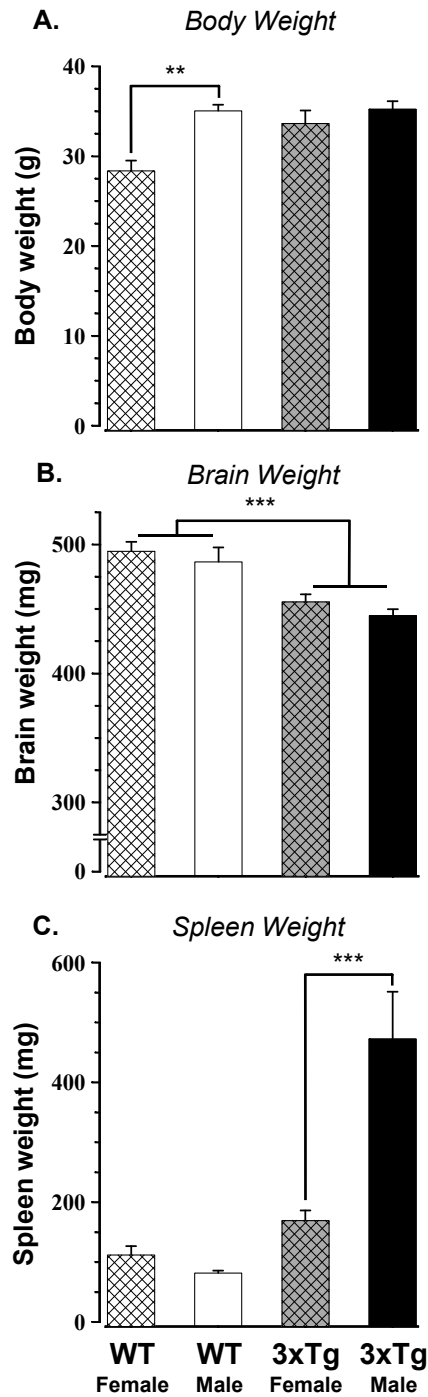


Figure 1 - Kapadia et al., 2017

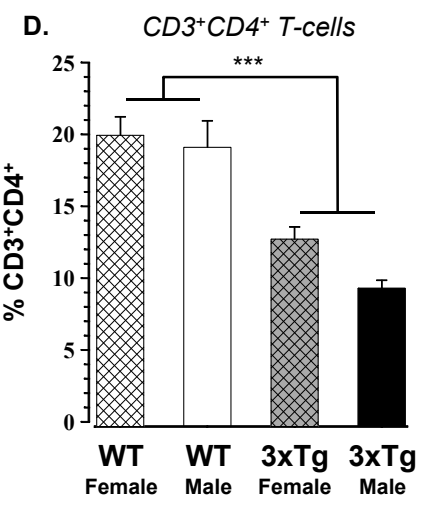
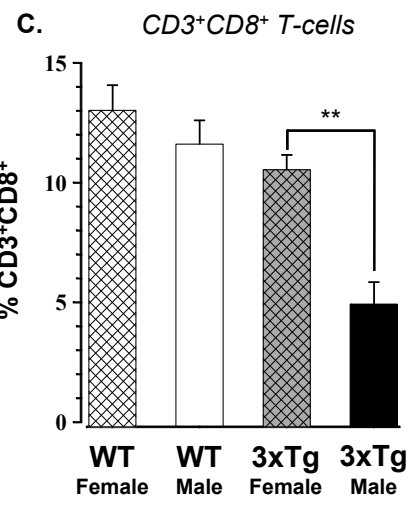
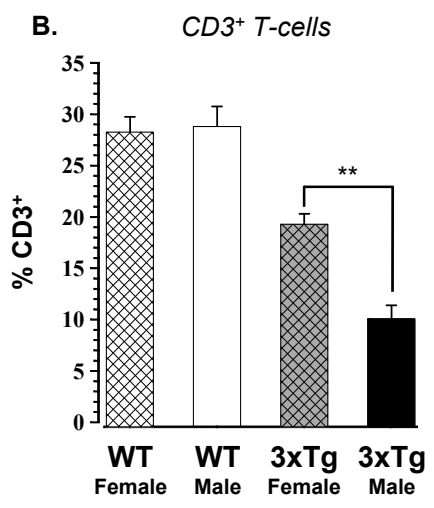
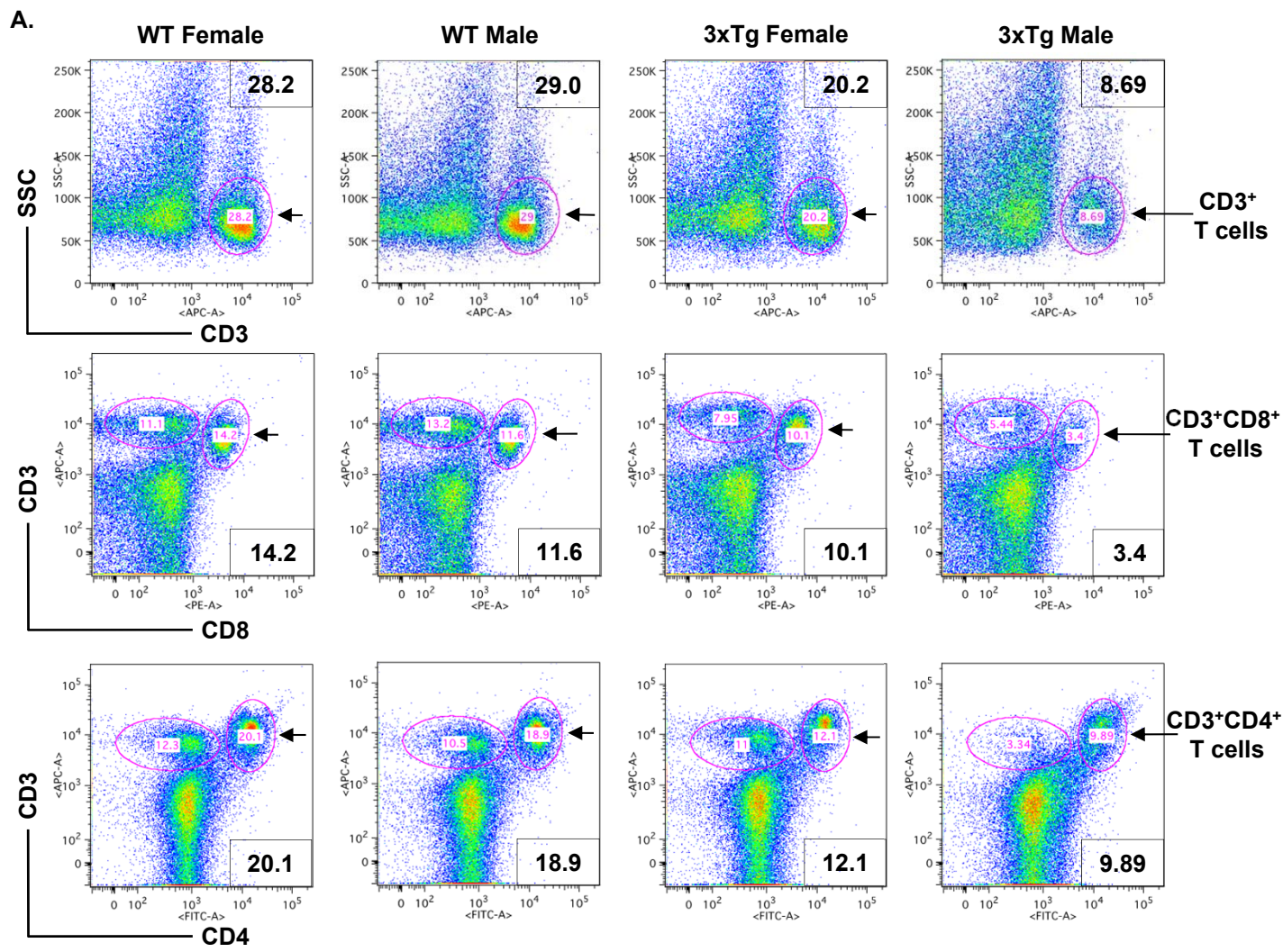


Figure 2 - Kapadia et al., 2017

A. Serum autoantibodies against cell nuclei

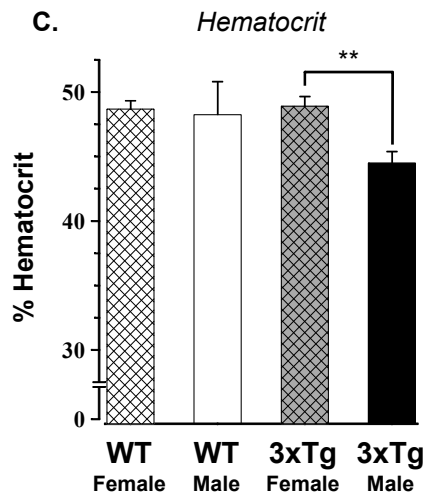
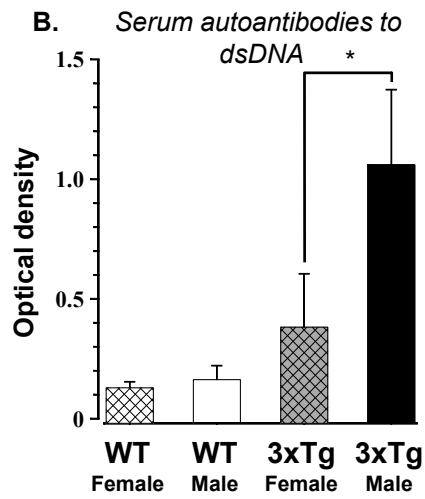
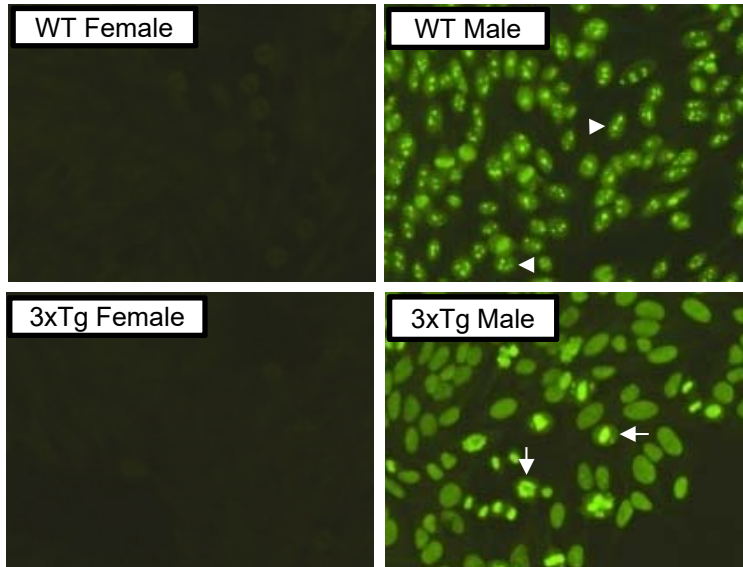


Figure 3 - Kapadia et al., 2017

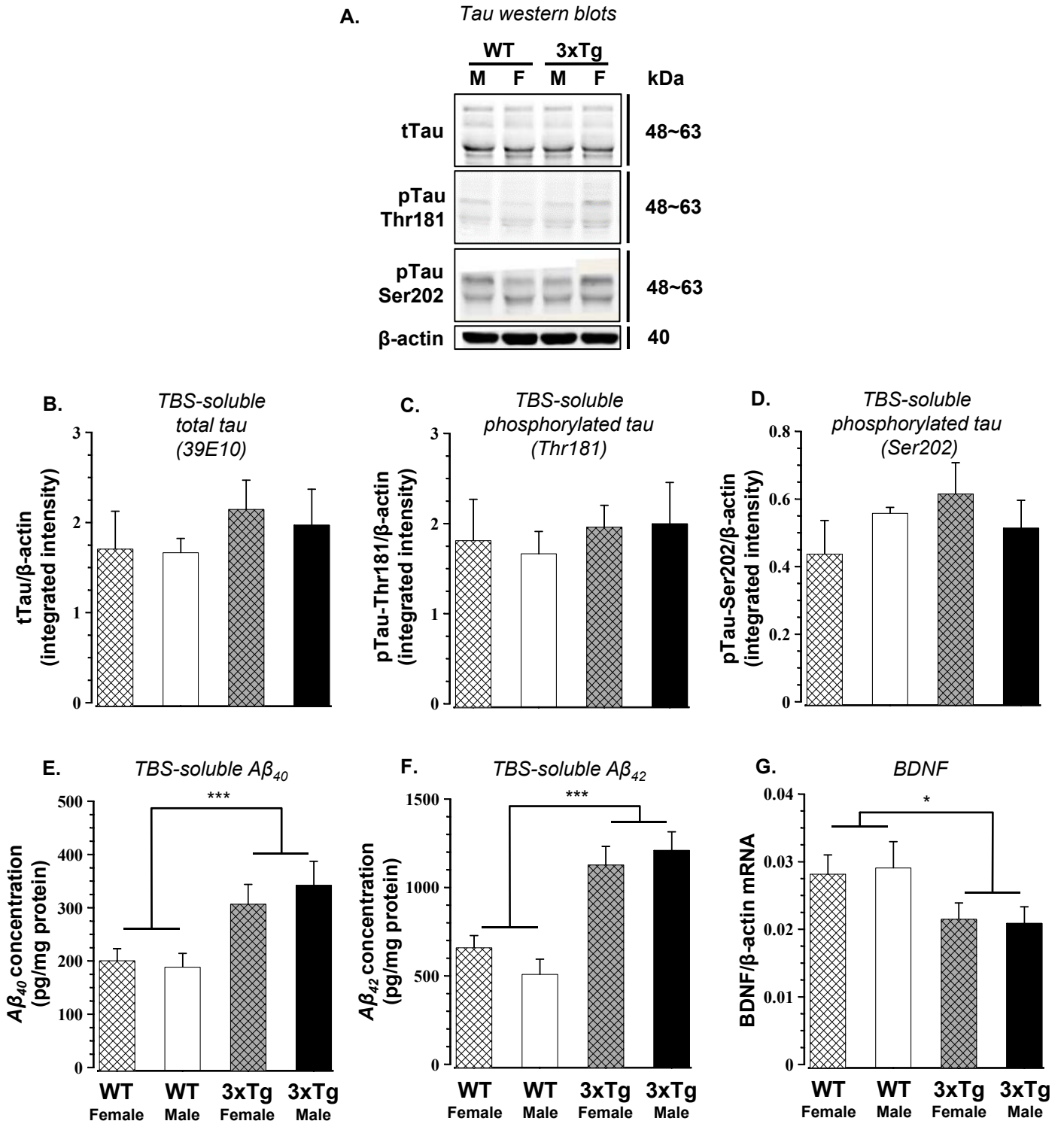


Figure 4 - Kapadia et al., 2017

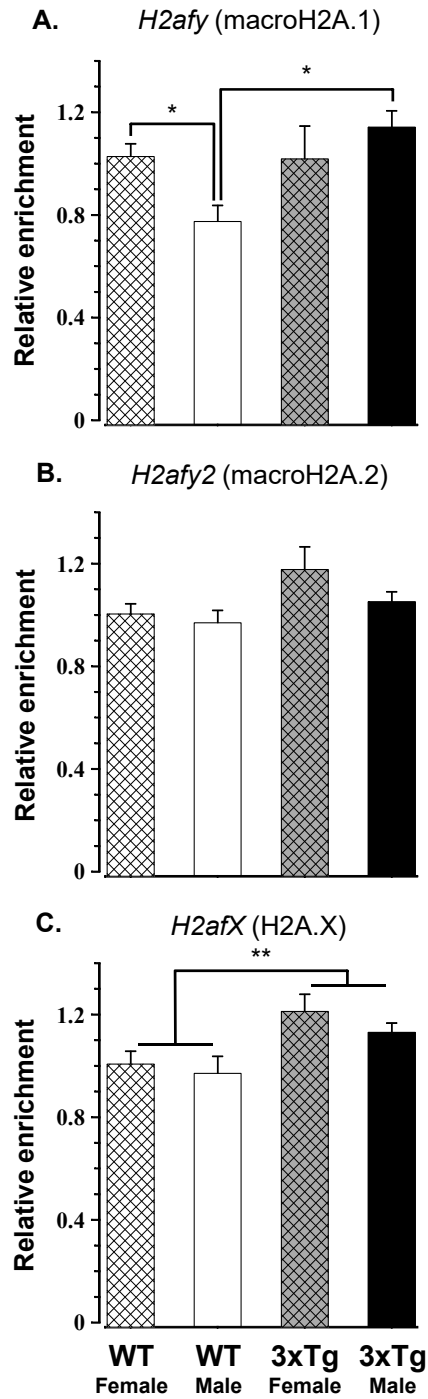


Figure 5 - Kapadia et al., 2017

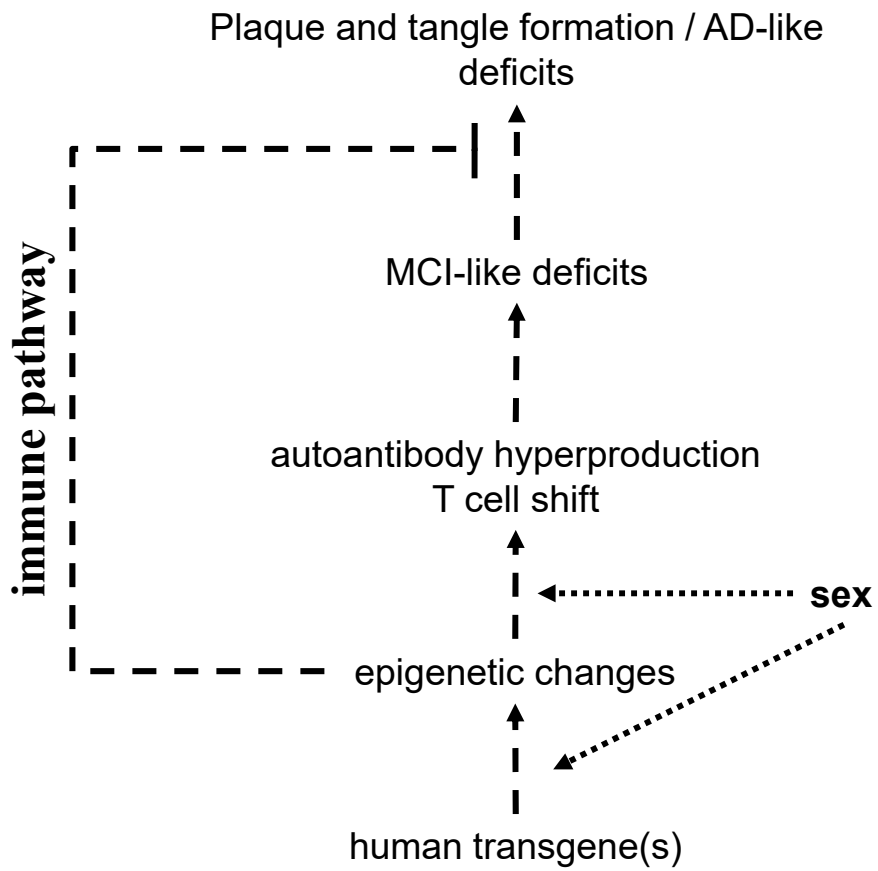


Figure 6 - Kapadia et al., 2017